Analysis of in-grain orientation distributions in deformed aluminium using X-ray diffraction and finite elements

Loïc Renversade, Romain Quey

Analysis of in-grain orientation distributions in deformed aluminium using X-ray diffraction and finite elements

To cite this article: Loïc Renversade and Romain Quey 2019 *IOP Conf. Ser.: Mater. Sci. Eng.* **580** 012022

IOP Conf. Series: Materials Science and Engineering **580** (2019) 012022 doi:10.1088/1757-899X/580/1/012022

Analysis of in-grain orientation distributions in deformed aluminium using X-ray diffraction and finite elements

Loïc Renversade and Romain Quey

Mines Saint-Etienne, Univ Lyon, CNRS, UMR 5307 LGF, Centre SMS, F – 42023 Saint-Etienne, France

E-mail: romain.quey@mines-stetienne.fr

Abstract. The lattice orientation distributions developing inside individual grains of a polycrystalline aluminium sample subjected to plastic deformation are analysed. In the experiment, diffraction contrast tomography (DCT) and far-field 3D X-ray diffraction microscopy (3DXRD) are used to track the development of the orientation distributions of 466 grains of an aluminium polycrystal deformed in tension to successive strains of 1.0, 1.5, 2.0, 2.5 and 4.5%. A new method is presented and employed to determine the in-grain orientation distributions from broadening of the diffraction spots. The polycrystal deformation is then simulated using the crystal-plasticity finite element method, starting from the initial, DCT-determined microstructure. The experimental and numerical in-grain lattice orientation distributions are analysed and compared in terms of trends over all grains and grain by grain.

1. Introduction

In-grain lattice orientation distributions develop inside grains of polycrystals subjected to plastic deformation and are important for subsequent annealing. Historically, these orientation distributions have been analysed destructively, by 2D EBSD [1, 2]. They are now accessible non-destructively, in 3D, using synchrotron X-ray diffraction [3, 4, 5]. Numerically, they can be simulated by crystal plasticity finite element simulations [2, 6]. This work focuses on the orientation distributions developing in individual grains of an Al–0.3wt% Mn polycrystal deformed to a few percent in tension, using a synchrotron X-ray diffraction experiment and finite element simulations. The development of the orientation distributions is analysed in terms of (angular) extent and anisotropy, i.e. development of a preferential disorientation direction. In Section 2, we describe the experiment and a new post-processing method to determine orientation distributions from far-field 3DXRD diffraction (simply referred to as "3DXRD" in the following) data. In Section 3, we describe the finite element simulation. In Section 4, we compare experiment and simulation in terms of trends over all grains and grain by grain, before closing the article with conclusions in Section 5.

2. Experiment

2.1. Data acquisition

A high-purity Al–0.3wt% Mn alloy with an average grain size of about 130 µm and a relatively weak initial crystallographic texture was used. A tensile specimen with a square section of

1×1 mm was cut for the tensile test. A combination of near-field and far-field X-ray diffraction techniques were used (figure 1a). For the initial state, the polycrystal structure was mapped using DCT (figure 1b), and, in the deformed state, the grain orientations were followed by 3DXRD [3] (figures 1c,d). DCT was applied on a region 1.4 mm high, while 3DXRD was applied on a central region 0.55 mm high. In both cases, diffraction images were acquired with an integration step of 0.1° (in ω) while the sample was continuously rotated by 360°. Having a DCT region significantly larger than the 3DXRD region later made it possible to avoid any bias caused by the boundary conditions of the finite element simulation (applied to the top and bottom surfaces of the DCT polycrystal) on the rotations of the grains of the central region. 3DXRD was carried out at successive strains of 1%, 1.5%, 2%, 2.5% and 4.5%. As will be seen in the following, not only the overall shifts of the diffraction spots (which are related to the average grain rotations) but also their broadening (which is related to the development of orientation distributions) were used. The DCT polycrystal contained 1848 grains, and the region analysed by 3DXRD contained 824 grains, 466 of which were followed during the entire deformation and will be used in the following.

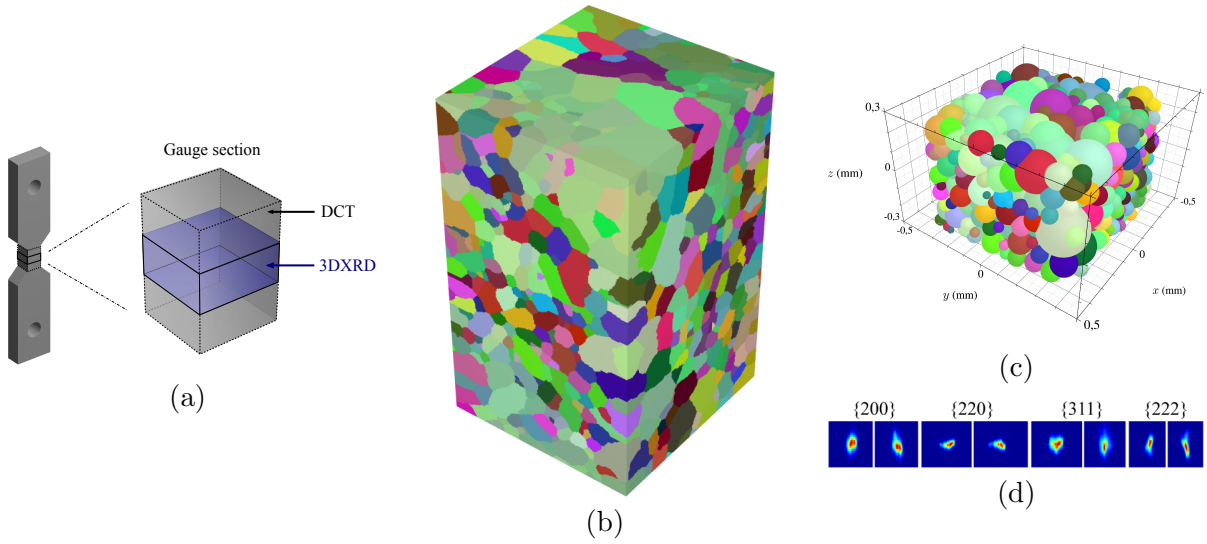

Figure 1. Principle and first results of the X-ray diffraction experiment. (a) Tensile specimen and observation regions, (b) initial microstructure obtained by DCT, (c) grains represented as spheres of equivalent volumes, obtained by 3DXRD, and (d) a series of diffraction spots of a particular grain (azimuthal projection, $\varepsilon = 4.5\%$).

2.2. Orientation distribution determination

The diffraction spots of a grain contain information on its lattice orientations (and elastic strains). As plastic deformation accumulates, diffraction spots broaden. Broadening occurs differently for different diffraction spots, but all diffraction spots result from the same orientation distribution. It should therefore be possible to determine an orientation distribution from the diffraction spots. Hansen et al. [7] proposed a direct, algebraic method to do so, but which, depending on the amount of data and unknowns, can become computationally very large and thus require the use of complex, iterative regularization methods. In this paper, we are mostly focused on the main properties of the orientation distributions, such as their angular extent and anisotropy (preferential disorientation directions). It should therefore be possible to consider a model orientation distribution, which takes these attributes into account using only a few parameters, and to determine the values of these parameters by optimization, by maximizing

the similarity between the experimental diffraction spots and the diffraction spots generated from the model orientation distribution.

For a given grain, all available experimental diffraction spots (identified at the grain indexation stage) are used to determine the grain orientation distribution, which corresponds to 40–100 spots. Diffraction spots are intrinsically 3D, as they are 2D on the detector (of directions $\boldsymbol{u}$ and $\boldsymbol{v}$) but also span several diffraction images while rotating the sample (in ω). However, the diffraction spots can be projected in their corresponding azimuthal planes (η, ω) to retain only the lattice orientation information.

Simulated spots are generated from the model orientation distribution. In general, at low-to-moderate strains, most grains develop a "unimodal" orientation distribution [8, 2], which can be represented by a three-variate normal distribution,

$$P(\boldsymbol{w}) = \prod_{i=1}^{3} \frac{1}{\sqrt{2\,\pi\,{\sigma_i}^2}} \exp\left(-\frac{{w'_i}^2}{2\,{\sigma_i}^2}\right), \tag{1}$$

where w'_i ($i = 1, 2, 3$) are the disorientations along the principal directions of the distribution and form vector $\boldsymbol{w'}$. σ_i ($i = 1, 2, 3$) are the standard deviations along the three principal directions. The three principal directions of the distribution are related to the laboratory directions by

$$\boldsymbol{w'} = \boldsymbol{K}\,\boldsymbol{w}, \tag{2}$$

where $\boldsymbol{K}$ is a rotation matrix, and $\boldsymbol{w}$ is the disorientation vector expressed in the laboratory directions. It follows that P depends on six parameters, which are the three standard deviations ($\sigma_1 \geq \sigma_2 \geq \sigma_3$) and three parameters describing $\boldsymbol{K}$ (in practice, the three Rodrigues vector components are used). For specified values of these parameters, the orientation distribution is discretized on a grid of size $[-3\,\sigma_i, 3\sigma_i]^3$, typically using 80 bins in each direction (which corresponds to a total of 512,000 bins), and the corresponding diffraction spots are generated (in azimuthal projection) for all experimental diffraction spots.

For each grain, experimental and simulated diffraction spots are compared one-to-one in terms of the Pearson product-moment correlation coefficient, r_k. The similarity between all experimental and simulated diffraction spots is then simply measured by

$$O = \frac{1}{n}\sum_{k=1}^{n} r_k, \tag{3}$$

where n is the number of diffraction spots. To determine the parameters of the model orientation distribution ($\sigma_{1\text{–}3}$ and $\boldsymbol{K}$), O is then maximized by gradient-free optimization, using NLopt's subplex algorithm [9, 10]. In average over all grains, optimization resulted in a value of O of 0.84, which confirms that orientation distributions can be well-approximated by three-variate normal distributions and validates the whole methodology.

In the following, orientation distributions will be described and analysed in terms of two metrics. The first metric is the angular extent, θ_d, which corresponds to the average disorientation angle with respect to the average orientation. θ_d is not among the orientation distribution parameters used previously, but we consider an expression of the form

$$\theta_d = \frac{2}{3}\sqrt{\frac{8}{\pi}}\,(\sigma_1 + \sigma_2 + \sigma_3), \tag{4}$$

which is equal to the expression proposed in Ref. [8] for an isotropic distribution ($\sigma_1 = \sigma_2 = \sigma_3$). The second metric is the preferential disorientation direction, $\boldsymbol{v_1}$, which is provided by the first row of $\boldsymbol{K}$ (the vector associated to σ_1).

3. Simulation

The initial, DCT microstructure was meshed following the methodology detailed in Refs. [11, 12] and implemented in the free (open-source) Neper software package, see figure 2a. Grains were finely discretized into tetrahedral elements, with an average mesh density of 600 elements per grain. The crystal plasticity finite element simulation of the polycrystal deformation was then carried out using the FEpX software package [13, 14]. Plastic deformation is accommodated by slip on the 12 $\{1\,1\,1\}\langle 1\,1\,0\rangle$ slip systems. On each system (α), the slip rate, $\dot{\gamma}^\alpha$, is related to the resolved shear stress, τ^α, by

$$\dot{\gamma}^\alpha \;=\; \dot{\gamma}_0 \,|\, \frac{\tau^\alpha}{g^\alpha} \,|^{\frac{1}{m}} \operatorname{sgn}(\tau^\alpha)\,, \qquad \dot{g}^\alpha \;=\; h_0 \left(\frac{g_s \;-\; g^\alpha}{g_s \;-\; g_0} \right)^{n'} \sum_\alpha |\dot{\gamma}^\alpha|. \tag{5}$$

The material parameters were identified from the experimental stress-strain behaviour, and their values are $\dot{\gamma}_0 = 1\ \mathrm{s}^{-1}$ (a convention), $m = 0.03$, $h_0 = 47$ MPa, $g_0 = 6$ MPa, $g_s = 455$ MPa and $n' = 2.6$. Figures 2b,c provide the rotation angles at $\varepsilon = 4.5\%$ (with respect to the initial orientation).

As in the experiment, the orientation distributions are analysed in terms of average extent (θ_d) and preferential disorientation direction ($\boldsymbol{v_1}$). For each grain, θ_d is readily computed from the grain elemental orientations, while the preferential disorientation direction ($\boldsymbol{v_1}$) is characterized by an eigendecomposition of the set of disorientations (represented as Rodrigues vectors) into eigenvectors ($\boldsymbol{v_i}$, $i = 1, 2, 3$) and eigenvalues ($\lambda_i = {\sigma_i}^2$, $\lambda_1 \geq \lambda_2 \geq \lambda_3$) [8]. Figure 2d shows the disorientation distribution corresponding to the grain of figure 2c, represented as Rodrigues vectors.

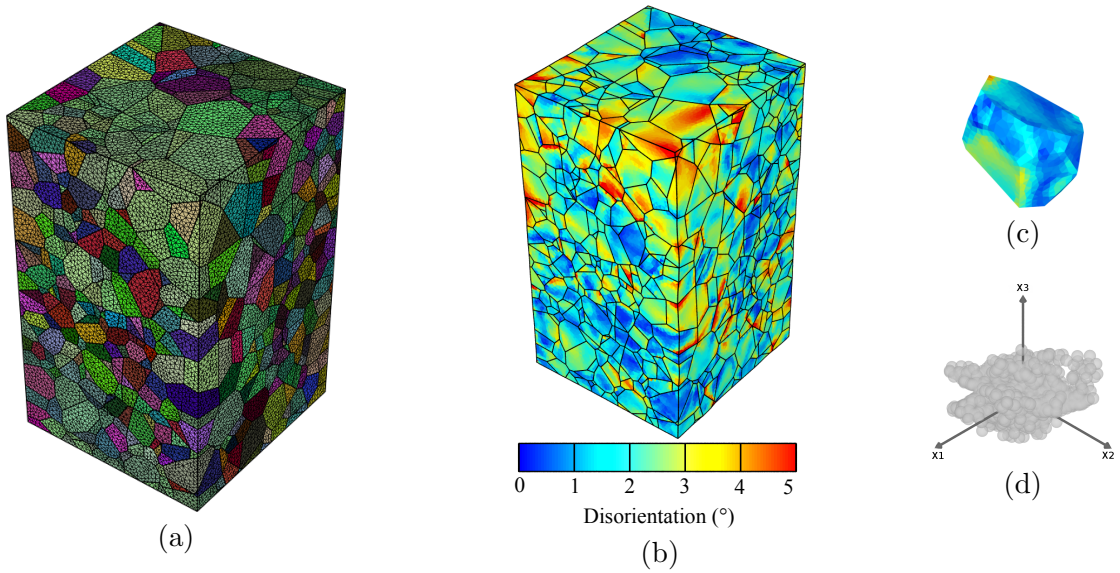

(a) (b) (c) (d)

Figure 2. Principle and first results of the finite element simulation. (a) mesh, (b) lattice rotation angle at 4.5% (with respect to the initial orientation), (c) lattice rotation angle at 4.5% for a particular grain, and (d) corresponding disorientation distribution in Rodrigues space. Note the distribution anisotropy.

4. Results and discussion

The distributions over all grains of the average disorientation angles are represented in figure 3. For both experiment and simulation, average disorientation angles increase gradually during

deformation, but also exhibit a high degree of variability, ranging, at $\varepsilon = 4.5\%$, in the experiment from 0.2° to 3.2° and in the simulation from 0.4° to 3.1°. Average values are, in the experiment, 0.18°, 0.24°, 0.31°, 0.34° and 0.61°, and, in the simulation, 0.17°, 0.27°, 0.37°, 0.46° and 0.77°. Figure 3c provides the correlation between the experimental and simulated average disorientation angles (θ_d), which show only moderate agreement.

The distributions over all grains of the preferential disorientation directions at successive strains are provided in figure 4 as equal-area projection onto the sample X–Y plane (Z = tensile direction), for both experiment and simulation. In the experiment, the preferential disorientation directions are first aligned with the tensile direction and then become perpendicular to it, mostly about direction X (figure 4a). In the simulation, the preferential disorientation directions are aligned with a direction close to X at all strains. (On figures 4a,b, the lack of uniaxial symmetry can simply be explained by the initial material texture.) A distribution of the preferential disorientation directions perpendicular to the tensile directions is consistent with an earlier study, made in hot plane strain compression, in which it was concluded that preferential disorientation directions align with the spin vectors of the most active slip systems [2]. In tension, most favorable slip systems have a spin vector oriented 90° away from Z, and so in the X–Y plane. Figure 4c provides the correlation between the experimental and simulated preferential disorientation directions at $\varepsilon = 4.5\%$, as the scalar product between the two. With an average value of 0.75, experimental and simulated preferential disorientation directions show

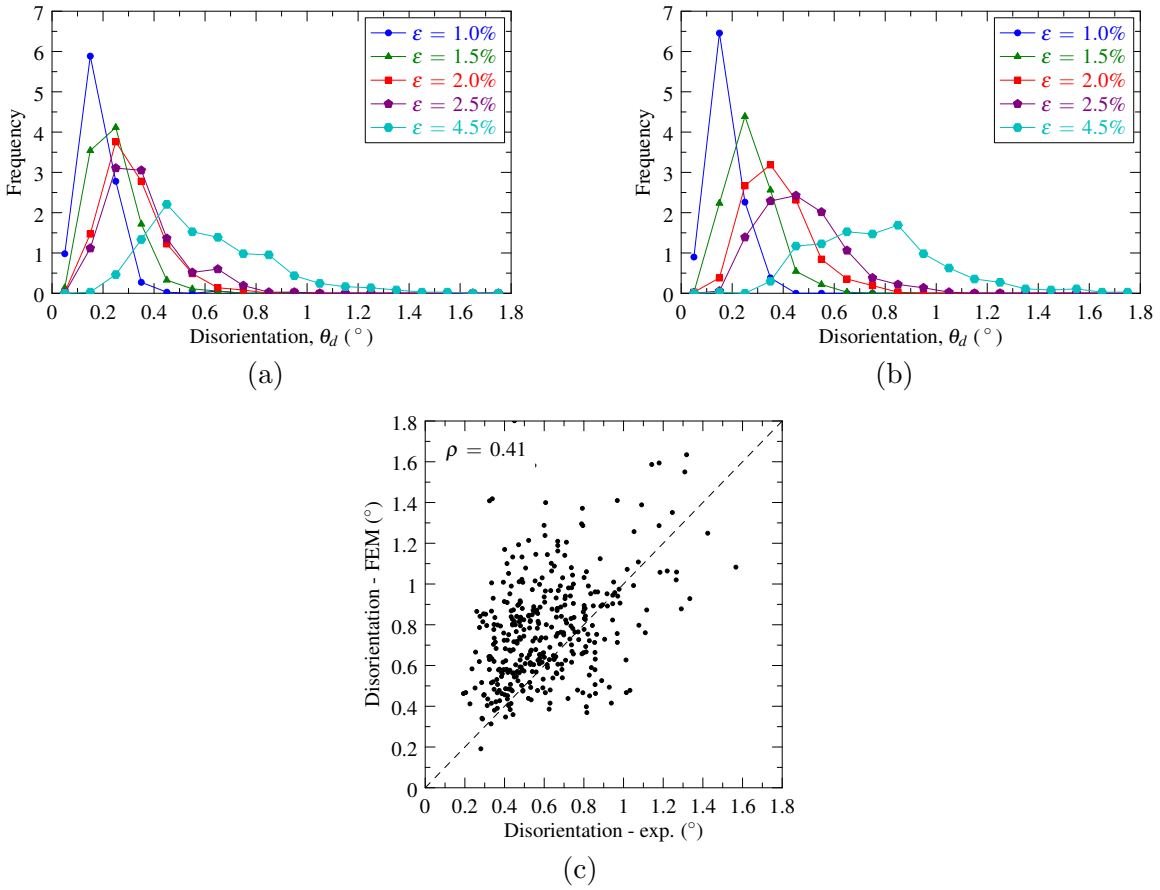

Figure 3. Distributions over all grains of the average disorientations, θ_d. (a) experiment, (b) simulation and (c) grain-by-grain comparison between experiment and simulation at $\varepsilon = 4.5\%$. ρ is the linear correlation coefficient.

an appreciable agreement.

A few more comments can be made about the comparison between experiment and simulation. In particular, it is seen that the grain-by-grain agreement on the average disorientation angles is relatively low (figure 3c) and that the distributions of the preferential disorientation directions at $\varepsilon = 1\%$ are different. This cannot be explained by experimental biases, such as a typical sample realignment toward the tensile direction at the beginning of deformation. Indeed, the average disorientation angles, as scalars, would not be affected, nor would be the in-grain preferential disorientation directions, as instantaneous, intragranular properties. (In contrast, sample realignment would affect the rotation directions with respect to the initial orientations.) Differences may actually be attributed to uncertainties on the crystal behaviour used in the simulation, whose parameters have been identified from the macroscopic behaviour. As for the distributions of the preferential disorientation directions at $\varepsilon = 1\%$, the differences may also be explained by the tendency of crystal-plasticity simulations to evolve microstructures too rapidly, as was also observed in [2].

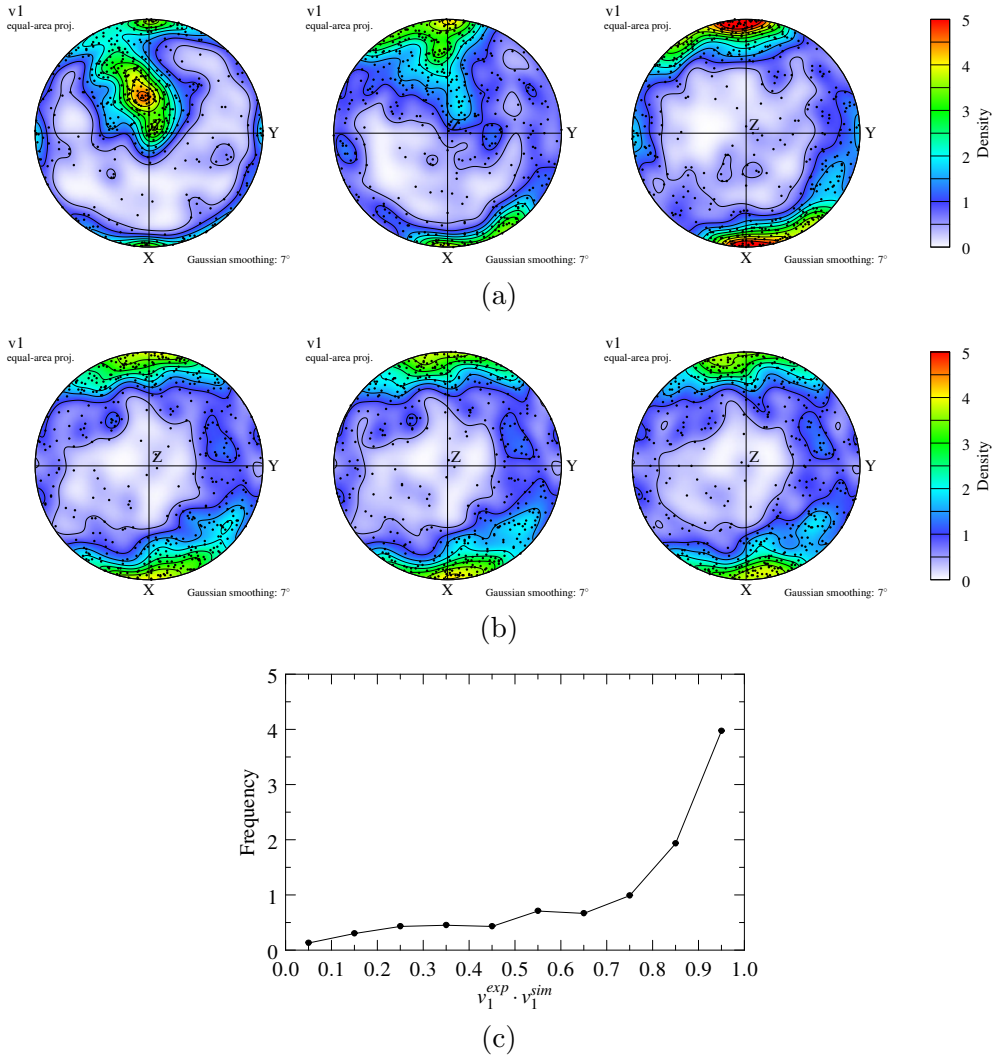

Figure 4. Distributions over all grains of the preferential disorientation directions, $\boldsymbol{v_1}$. (a) experiment and (b) simulation at strains of 1%, 2% and 4.5% (left to right). Z represents the tensile direction. (c) Distribution of the correlations between the experimental and simulated preferential disorientation directions ($\boldsymbol{v_1}^{\text{exp}}$ and $\boldsymbol{v_1}^{\text{sim}}$, respectively) at 4.5%.

5. Conclusions

The orientation distributions developed within individual grains of an aluminium polycrystal were experimentally characterized using a new far-field 3DXRD based method and numerically simulated using the finite element method. Results were obtained on a statistically-representative set of 466 grains. The new 3DXRD based method was particularly efficient in determining the orientation distribution from several tens of diffraction spots represented in azimuthal projection. The results, analysed in terms of angular extent (average disorientation angle, θ_d) and preferential disorientation direction ($\boldsymbol{v_1}$), were analysed. A high degree of variability among grains was found, which was well reproduced by the simulation. Trends over all grains were in agreement with previous observations made in hot plane strain compression [2]. In particular, preferential disorientation directions are found to align with the spin vectors of the typically most active slip systems. On a grain-by-grain basis, experiment and simulation were found in appreciable agreement on the preferential disorientation directions ($\boldsymbol{v_1}$).

6. Acknowledgments

W. Ludwig, J. Wright and A. Borbély are acknowledged for help during the experiment.

References

[1] Humphreys F and Bate P 2007 *Acta Mater.* **55** 5630–45
[2] Quey R, Driver J and Dawson P 2015 *J. Mech. Phys. Solids* **84** 506–27
[3] Poulsen H, Margulies L, Schmidt S and Winther G 2003 *Acta Mater.* **51** 3821–30
[4] Pokharel R, Lind J, Kanjarla A, Lebensohn R, Fai Li S, Kenesei P, Suter RM and Rollett A 2014 *Annu. Rev. Condens. Matter Phys* **5** 317–46
[5] Viganò N, Tanguy A, Hallais S, Dimanov A, Bornert M, Batenburg K and Ludwig W 2016 *Sci. Rep.* **6**
[6] Quey R, Dawson P and Driver J 2012 *J. Mech. Phys. Solids* **60** 509–24
[7] Hansen C, Sørensen H, Sükösd Z and Poulsen H 2009 *SIAM J. Imaging Sci.* **2** 593–613
[8] Glez J C and Driver J 2003 *Acta Mater.* **51** 2989–3003
[9] Johnson S *http://ab-initio.mit.edu/wiki/index.php/NLopt*
[10] Rowan T 1990 *Functional Stability Analysis of Numerical Algorithms* Ph.D. thesis
[11] Quey R and Renversade L 2018 *Comp. Methods Appl. Mech. Eng.* **330** 308–33
[12] Quey R, Dawson P and Barbe F 2011 *Comput. Methods Appl. Mech. Eng.* **200** 1729–45
[13] Marin E and Dawson P 1998 *Comput. Methods Appl. Mech. Eng.* **165** 1–21
[14] Dawson P and Boyce D 2015 *ArXiv* arXiv:1504.03296 [cond–mat.mtrl–sci]